

An Adaptive Optimizer for Measurement-Frugal Variational Algorithms

Jonas M. Kübler,^{1,2} Andrew Arrasmith,¹ Lukasz Cincio,¹ and Patrick J. Coles^{1,*}

¹*Theoretical Division, MS 213, Los Alamos National Laboratory, Los Alamos, NM 87545, USA.*

²*Max Planck Institute for Intelligent Systems, Max-Planck-Ring 4, 72076 Tübingen, Germany.*

Variational hybrid quantum-classical algorithms (VHQCAs) have the potential to be useful in the era of near-term quantum computing. However, recently there has been concern regarding the number of measurements needed for convergence of VHQCAs. Here, we address this concern by investigating the classical optimizer in VHQCAs. We introduce a novel optimizer called individual Coupled Adaptive Number of Shots (iCANS). This adaptive optimizer frugally selects the number of measurements (i.e., number of shots) both for a given iteration and for a given partial derivative in a stochastic gradient descent. We numerically simulate the performance of iCANS for the variational quantum eigensolver and for variational quantum compiling, with and without noise. In all cases, and especially in the noisy case, iCANS tends to out-perform state-of-the-art optimizers for VHQCAs. We therefore believe this adaptive optimizer will be useful for realistic VHQCA implementations, where the number of measurements is limited.

I. INTRODUCTION

There are various strategies to make use of noisy intermediate-scale quantum (NISQ) computers [1]. One particularly promising strategy is to push most of the algorithmic complexity onto a classical computer while running only a small portion of the computation on the NISQ device. This is the idea behind variational hybrid quantum-classical algorithms (VHQCAs) [2]. VHQCAs employ a quantum computer to efficiently estimate a cost function that depends on the parameters of a quantum gate sequence, and then leverage a classical optimizer to minimize this cost. VHQCAs intend to achieve a quantum advantage with NISQ computers by finding short-depth quantum circuits that at least approximately solve some problem. VHQCAs have been proposed for many applications including ground-state preparation, optimization, data compression, simulation, compiling, factoring, diagonalization, and others [3–20].

A concern about VHQCAs is that they might require prohibitively many quantum measurements (shots) in order to achieve convergence of the cost function [21], especially for applications like quantum chemistry that require chemical accuracy [22, 23]. In response to this concern, there has been a recent explosion of papers looking to improve the measurement frugality of VHQCAs by simultaneously measuring commuting subsets of the Pauli operators needed for the cost function [24–30].

Here, we approach the problem from a different direction by aiming to improve the classical optimizer. There have been several recent efforts to improve optimizers for VHQCAs [31–35]. Our approach is different from these works in that the optimizer we propose is specifically constructed to achieve measurement frugality. In particular, we develop an adaptive optimizer that is adaptive in two senses: it frugally adjusts the number of shots for a given iteration and for a given partial derivative.

Our method is inspired by the classical machine learning algorithm named Coupled Adaptive Batch Size (CABS) [36]. For pedagogical reasons, we first directly adapt the CABS algorithm to VHQCA applications and call the resulting algorithm Coupled Adaptive Number of Shots (CANS). In order to achieve greater measurement frugality, we go beyond direct adaptation and modify the optimizer to account for differences in the number of shots needed to estimate individual components of the gradient. We call this method individual-CANS (iCANS).

While iCANS is conceptually simple, it nevertheless performs very well. Using IBM’s simulator [37], we implement iCANS and other state-of-the-art optimizers such as Adam [38], SPSA [39], and sequential gate optimization [33, 34] for both the variational quantum eigensolver [3] and variational quantum compiling [14–17]. We find that iCANS on average performs the best. This is especially true for our implementations in the presence of noise, i.e., with IBM’s simulator of their NISQ device. This is encouraging since VHQCAs must be able to run in the presence of noise to be practically useful.

Ultimately, one can take a multi-pronged approach to reducing measurements in VHQCAs, e.g., by combining our measurement-frugal classical optimizer with the recent advances on Pauli operator sets in Refs. [24–30]. However, one can apply our optimizer to VHQCAs that do not involve the measurement of Pauli operator sets (e.g., the VHQCAs in [7–9]). In this sense, our work is relevant to all VHQCAs.

In what follows, we first give a detailed review of various optimizers used in the classical machine learning and quantum circuit learning literature. We remark that this lengthy review aims to assist readers who may not have a background in classical optimization, as this article is intended for a quantum-computing audience. (Experienced readers can skip to Section III.) We then present our adaptive optimizer, followed by the results of our numerical implementations.

* pcoles@lanl.gov

II. BACKGROUND

A. Gradient Descent

One standard approach to minimization problems is gradient descent, where the optimizer iteratively steps along the direction in parameter space that is locally “downhill” (i.e., decreasing) for some function $f(\boldsymbol{\theta})$. Mathematically, we can phrase the step at the t -th iteration as

$$\boldsymbol{\theta}^{(t+1)} = \boldsymbol{\theta}^{(t)} - \alpha \nabla f(\boldsymbol{\theta}^{(t)}), \quad (1)$$

where α is called the *learning rate*. If one takes a large learning rate, one cannot be sure that one will not go too far and possibly end up at a higher point. For a small learning rate one is more guaranteed to keep making incremental progress (assuming the change in slope is bounded), but it will take much longer to get to a minimum. Knowing an upper bound on the slope is therefore very helpful in determining the appropriate learning rate.

To formalize this discussion, we review the notion of Lipschitz continuous gradients. The gradient of a function f is Lipschitz continuous if there exists some L (called the Lipschitz constant) such that

$$\|\nabla f(\boldsymbol{\theta}^{(t+1)}) - \nabla f(\boldsymbol{\theta}^{(t)})\| \leq L \|\boldsymbol{\theta}^{(t+1)} - \boldsymbol{\theta}^{(t)}\|, \quad (2)$$

for all $\boldsymbol{\theta}^{(t+1)}$ and $\boldsymbol{\theta}^{(t)}$. (We note that in our notation the $\|\cdot\|$ without a subscript denotes the ℓ_2 or Euclidean norm.) When this holds, we can see that the fractional change in the gradient over the course of one step is bounded by αL , meaning that for sufficiently small α we can be sure that we are following the gradient. In fact, the convergence of the basic gradient descent method is guaranteed for deterministic gradient evaluations so long as $\alpha < 2/L$ [36]. In machine learning contexts L is usually unknown, but for VHQCs it is often possible to determine a good bound. We discuss this alongside an analytic formula for estimating gradients for VHQCs in the next subsection.

B. Gradient Estimation

Working with the exact gradient is often difficult for two reasons. First the gradient can depend on quantities that are expensive to estimate with high precision. Second, it might be that no analytic form for the gradient formula is accessible, and hence the gradient must be approximated by finite differences. In the following we discuss the two scenarios in more detail.

1. Analytic gradients

If one has sufficient knowledge of the structure of the optimization problem under consideration, it might be

possible to find analytic expressions for the gradient of the function. In deep learning this is what is provided via the backpropagation algorithm, which allows one to take analytic derivatives with respect to all parameters [40]. However these formulas are usually expressed as an average over the full sample one has available in a learning task. To decrease the cost of evaluating the gradient often only a subset of the full sample, a so-called mini-batch, is used to get an unbiased estimate of the gradient [40]. This introduces a trade-off between the cost of the gradient estimation and its achieved precision.

In VHQCs there exist similar scenarios where it is possible to analytically compute the gradients [41–43]. For example if the parameters describe rotation angles of single-qubit rotations and the cost function is the expectation value of some operator \mathbf{A} , $f = \langle \mathbf{A} \rangle$, partial derivatives can be computed as

$$\partial_{\theta_i} f(\boldsymbol{\theta}) = \frac{f(\boldsymbol{\theta} + \frac{\pi}{2} \hat{e}_i) - f(\boldsymbol{\theta} - \frac{\pi}{2} \hat{e}_i)}{2}, \quad (3)$$

i.e., the partial derivative is determined by the value of the cost function if one changes the i -th component by $\pm\pi/2$. However, the value of the cost function can only be estimated from a finite number of measurements, and this number of measurements as well as the noise level of the computation itself determine the precision of the gradient estimates. Therefore it is important to understand how to choose the number of shots, and keep in mind that for VHQCs the gradient estimate is always noisy to some extent, even though it is referred to as analytical.

An immediate extension of this is that (3) can be used recursively to define higher derivatives. This result then allows one to determine a usefully small upper bound on L in (2). In particular, we note for operators with bounded eigenspectra, the largest magnitude of a derivative of any order we can find with (3) is precisely half the difference between the largest and smallest eigenvalues λ_{\max} and λ_{\min} , respectively. Thus,

$$L \leq \frac{\lambda_{\max} - \lambda_{\min}}{2}. \quad (4)$$

For the common case where the eigenspectrum is unknown but we know how to decompose \mathbf{A} into a weighted sum over tensor products of Pauli matrices, $\mathbf{A} = \sum_i a_i \boldsymbol{\sigma}_i$, we can bound the highest and lowest eigenvalues in turn by $\sum_i |a_i|$ and $-\sum_i |a_i|$, respectively, which gives

$$L \leq \sum_i |a_i|. \quad (5)$$

By setting equality in (5) (or (4) when we have more information), we therefore find a useful Lipschitz constant.

2. Finite Differencing

If one does not have access to analytical gradients, one way to approximate the partial derivatives is by taking a

finite δ step in parameter space

$$\partial_{\theta_i} f(\boldsymbol{\theta}) \approx \frac{f(\boldsymbol{\theta} + \delta \hat{e}_i) - f(\boldsymbol{\theta} - \delta \hat{e}_i)}{2\delta}. \quad (6)$$

Again, as in the analytical case, the function values need to be estimated by a finite number of shots introducing statistical noise. However, as opposed to the analytic case, the estimate (6) is systematically wrong, with an error that scales with δ^2 . Therefore, one might want to decrease the parameter δ during an optimization procedure using such a gradient estimate. Intuitively this makes the optimization harder, and was recently discussed in the context of VHQCAs [44].

C. Noisy Gradient Descent

For the case where one have noise in one's measurement of the gradient, the analysis of a gradient descent procedure becomes more complicated as the best one can achieve are statements about the behavior that can be expected on average. However, so long as one's estimates are unbiased (i.e., repeated estimates average to the true gradient) one should still end up near a minimum. This idea is at the heart of all stochastic gradient descent methods which we discuss now.

1. Stochastic/Mini-Batch Gradient Descent

In cases such as VHQCAs (as well as some machine learning applications), we cannot access the gradients directly and therefore need to estimate the the gradients by sampling from some distribution. A standard approach to this case is to choose some number of samples that are needed to achieve a desired precision. This method is known as either stochastic or mini-batch gradient descent. (A mini-batch here refers to a collection of samples, usually much smaller than the total population.)

The number of samples as well as the learning rate are usually set heuristically, in order to balance competing interests of efficiency and precision. First, when collecting samples is computationally expensive, it can sometimes be more efficient to take less accurate gradient estimates in order to converge faster, though doing so can be detrimental if it means that one ends up needing to perform an inordinate number iterations [45]. Second, it does not make sense to attempt to achieve a precision greater than intrinsic accuracy of the distribution from which one samples. If there is some error expected in the representation of the distribution one samples the gradients from, there is therefore an upper bound on the number of samples that it is sensible to take based on that accuracy [45]. For the case of VHQCAs, this often means that the upper limit on the number of samples, s_{\max} depends on the (usually unknown) bias b_{noise} introduced to the gradient measurements by the noise of the

physical quantum device:

$$s_{\max} \simeq \frac{\text{Var}(f(\boldsymbol{\theta}))}{b_{\text{noise}}^2(\boldsymbol{\theta})}. \quad (7)$$

Since for VHQCAs this bias is a function of the unknown, time varying device noise for the specific gate sequence, often the best one can do is to make a rough estimate about its order of magnitude and use that in the denominator.

Typically, the number of samples as well as the learning rate are heuristically adjusted based on the structure of the cost landscape as well as the error level. When little information is known about the optimization problem, the minimization process is optimized either by manual trial and error until an acceptable choice is found or using a hyper-parameter optimization strategy [46].

For a stochastic gradient approach to converge quickly, it is often helpful to decrease the error in the optimization steps during the run of the optimization. This can be done by either decreasing the learning rate α , or minimizing the noise in the gradient estimates. The following two subsections introduce two methods from machine learning that respectively take these two strategies.

2. Adam

Adam is a variant of stochastic gradient in which the step that is taken along each search direction is adapted based on the first and second moment of the gradient [38]. To do this, one takes an exponential decaying average of the first and second moment (m_t and v_t , respectively) for each component of the gradient individually

$$m_t = \beta_1 m_{t-1} + (1 - \beta_1) g_t \quad (8)$$

$$v_t = \beta_2 v_{t-1} + (1 - \beta_2) g_t^2, \quad (9)$$

where the square is understood element-wise, g_t is the gradient estimate at step t , and β_1, β_2 are the constants that determine how slowly the variables are updated. The parameters are then updated with the following rule:

$$\boldsymbol{\theta}^{(t+1)} = \boldsymbol{\theta}^{(t)} - \alpha \frac{\hat{m}_t}{\sqrt{\hat{v}_t + \epsilon}}, \quad (10)$$

where \hat{m}_t (\hat{v}_t) is an initialization-bias-corrected version of m_t (v_t), and ϵ is a small constant to ensure stability [38]. One particular feature of Adam is that the adaptation happens individually for each component of the gradient. We also briefly mention that there is a recent modification to Adam that looks promising, called Rectified Adam (RAdam) [47]. RAdam essentially selectively turns on the adaptive learning rate once the variance in the estimated gradient becomes small enough.

While Adam has made a large impact in deep learning, to our knowledge it has not been widely considered in the context of VHQCAs.

3. CABS

Balles et al. analyzed the problem of choosing the sample size in the context of optimizing neural networks by stochastic gradient descent [36]. Their approach is to find the number of samples s that maximizes the expected gain per sample at each iteration.

In the following we denote the i -th component of the estimated gradient by g_i , the empirical variance of the estimate g_i by S_i , the actual gradient by ∇f , and the actual covariance matrix (in the limit of infinite samples or shots) of the gradient estimation by Σ . Balles et al. introduce a lower bound \mathcal{G} on the gain (improvement in the cost function) per iteration. Accounting for the finite sampling error, they find that the average value of \mathcal{G} is [36]

$$\mathbb{E}[\mathcal{G}] = \left(\alpha - \frac{L\alpha^2}{2} \right) \|\nabla f\|^2 - \frac{L\alpha^2}{2s} \text{Tr}(\Sigma). \quad (11)$$

As an immediate consequence, they then find that the expected gain at any step has a positive lower bound if

$$\alpha \leq \frac{2\|\nabla f\|^2}{L(\|\nabla f\|^2 + \text{Tr}(\Sigma)/s)}. \quad (12)$$

By taking a small but fixed α , Balles et al. then maximize the lower bound on the expected gain per sample by taking

$$s = \frac{2L\alpha}{2 - L\alpha} \frac{\text{Tr}(\Sigma)}{\|\nabla f\|^2} \quad (13)$$

samples [36]. Unfortunately, this formula depends on quantities Σ and ∇f that are not accessible. Therefore in CABS, Σ is replaced by an estimator $\hat{\Sigma}$ and, specializing to the case where the minimum value of f is known to be zero, $\|\nabla f\|^2$ is replaced by f/α as the gradient estimator is biased. Since the Lipschitz constant is also often unknown in the machine learning problems they were considering, they also drop the factor of $2L\alpha/(2 - L\alpha)$ [36]. CABS then proceeds as a stochastic gradient descent with a fixed learning rate and a number of samples that is selected at each iteration based on (13) with the quantities measured at the previous point, making the assumption that the new point will be similar to the old point.

As discussed in the next section, our adaptive optimizer for VHQAs is built upon the ideas behind CABS (particularly (13)), although our approach differs somewhat.

D. SPSA Algorithm

The simultaneous perturbation stochastic approximation (SPSA) algorithm [39] is explicitly designed for a setting with only noisy evaluation of the cost function,

where no analytic formulas for the gradients are available. It is also a descent method, however, instead of estimating the full gradient, a random direction is picked and the slope in this direction is estimated. Based on this estimate a downhill step in the sampled direction is taken:

$$\boldsymbol{\theta}^{(t+1)} = \boldsymbol{\theta}^{(t)} - \alpha_t \mathbf{g}(\boldsymbol{\theta}^{(t)}). \quad (14)$$

Here $\mathbf{g}(\boldsymbol{\theta}^{(t)})$ is the estimated slope in the random direction and estimated as [48]:

$$\mathbf{g}(\boldsymbol{\theta}^{(t)}) = \frac{f(\boldsymbol{\theta}^{(t)} + c_t \boldsymbol{\Delta}_t) - f(\boldsymbol{\theta}^{(t)} - c_t \boldsymbol{\Delta}_t)}{2c_t} \boldsymbol{\Delta}_t^{-1}, \quad (15)$$

where $\boldsymbol{\Delta}_t$ is the random direction sampled for the t -th step and $\boldsymbol{\Delta}_t^{-1}$ simply denotes the vector with its element-wise inverses. In order to ensure convergence the finite difference parameter c_t as well as the learning rate α_t have to be decreased over the optimization run. This is commonly done by using a prefixed schedule [48]. In the original formulation, the idea is usually to estimate the cost function in (15) by a single measurement. However, in a quantum setting it seems intuitive to take a larger number of measurements for the estimation, as was done in [49].

E. Sequential Subspace Search

Another approach to optimizing a multivariate cost function is to break the problem into sub-parts which are independently easier to handle. The generic idea is to define a sequence of subspaces of parameter space to consider independently. These methods then approach a local minimum by iteratively optimizing the cost function on each subspace in the sequence. Now we discuss two instances of this approach: the famous Powell method [50] as well as a recently proposed method specialized to VHQAs [33, 34].

1. Powell Algorithm

The Powell algorithm [50] is a very useful gradient-free optimizer that specializes the subspace search to the case of sequential line searches. Specifically, starting with some input set of search vectors $V = \{\mathbf{v}_i\}$ (often the coordinate basis vectors of the parameter space) this method sequentially finds the set of displacements $\{a_i\}$ along each search vector that minimizes the cost function. Next, the method finds the \mathbf{v}_j associated with the greatest displacement, $a_j = \max(a_i)$. This \mathbf{v}_j is then replaced with the total displacement vector for this iteration, namely:

$$\mathbf{v}_j \rightarrow \sum_i a_i \mathbf{v}_i, \quad (16)$$

and then the next iteration begins with this updated set of search vectors. This replacement scheme accelerates

the convergence and prevents the optimizer from being trapped in a cyclic pattern. In practice, the displacements a_i are typically found using Brent’s method [51], but in principle any gradient-free scalar optimizer could work. (Gradient-based scalar optimizers would make Powell’s method no longer “gradient-free.”)

2. Sequential Optimization by Function Fitting

In the special case of VHQCAs where the cost function is expressed as an expectation value of some Hermitian operator and the quantum circuit is expressed as fixed two-qubit gates and variable single-qubit rotations, it is possible to determine the functional form of the cost function along a coordinate axis [33]. After fitting a few parameters, it becomes possible to compute where the analytic minimum should be to find the displacement along any given search direction. This can be scaled up to finding the analytic minimum (exact up to distortions from noise) on some subspace that is the Cartesian product of coordinate axes, though this is hampered by the fact that the number of parameters that must be fit scales exponentially with the dimension of the subspace [33]. We will refer to this algorithm as the Sequential Optimization by Function Fitting (SOFF) algorithm, and note that a very similar method that made small modifications was published shortly after SOFF [34].

We note that, though they are closely related, due to the limitation to only searching along coordinate axes, it is not possible to take arbitrary search directions, thus SOFF is not quite a special case of Powell’s method. For VHQCA problems where it is applicable, SOFF has been demonstrated to be highly competitive with or better than other standard optimization schemes like Powell’s method [33, 34].

III. ADAPTIVE SHOT NOISE OPTIMIZER

As mentioned above, the basic idea behind our approach is similar to that of CABS [36], but we implement those ideas in a different way. Specifically, by implementing different estimates for the inaccessible quantities in (13) that are suitable to the number of shots in a VHQCA (rather than the batch size in a machine learning method), we arrive at a variant of CABS we name *Coupled Adaptive Number of Shots* (CANS). Recognizing that a different number of shots might be optimal for estimating each component of the gradient in VHQCAs, we further develop this variation into *individual-CANS* (iCANS), which is our main result. For pedagogical purposes, we first introduce CANS and then present iCANS.

A. CANS

We now discuss our adaptation of CABS to the setting of VHQCAs. In order to use the number of shots recommended by the CABS method, we need to rewrite (13) using only quantities that are accessible. An unbiased estimate of $\text{Tr}(\Sigma)$ is given by $\sum_{i=1}^l S_i = \|S\|_1$, i.e., by the empirical variances of the gradient components. The naive estimate of $\|\nabla f\|^2$ is $\|g\|^2$, with $g := (g_1, \dots, g_l)^T$ the estimated gradient. This estimator is biased (see Equation (17) of [36]), however using a bias-corrected version is numerically unstable. With these choices, we then define CANS as the CABS algorithm with (13) replaced by

$$s = \frac{2L\alpha}{2 - L\alpha} \frac{\|S\|_1}{\|g\|^2}. \quad (17)$$

The CANS algorithm is included in Appendix A for completeness. For the remainder of the paper we will focus on iCANS, which we introduce next.

B. iCANS

The CANS algorithm is inspired by CABS [36], which was designed for applications in deep learning. Therein for each data point the full gradient is evaluated, and noise arises by considering only a minibatch of the full sample. In VHQCAs, however, each individual partial derivative is estimated independently on its own. This gives us the freedom to distribute measurements over the estimation of the partial derivatives more effectively. This is the idea behind iCANS, which is shown in Algorithm 1 and described below.

To prioritize the partial derivatives rather than the gradient magnitude as in (11), we introduce the expected lower bound on the *gain* per shot for each partial derivative *individually*

$$\gamma_i := \frac{\mathbb{E}[G_i]}{s_i} = \frac{1}{s_i} \left[\left(\alpha - \frac{L\alpha^2}{2} \right) g_i^2 - \frac{L\alpha^2}{2s_i} S_i \right], \quad (18)$$

where s_i is the suggested number of measurements for the estimation of the i -th partial derivative given by

$$s_i = \frac{2L\alpha}{2 - L\alpha} \frac{S_i}{g_i^2}. \quad (19)$$

The idea now is to update each parameter with a gradient descent step, where each partial derivative is estimated with its individual optimal number of measurements. However, empirically those parameters that are close to a local optimal value (hence have a small expected gain) require a large number of shots, while parameters that are far from convergence (and hence usually have a large expected gain) require a small number of shots. We therefore introduce an upper bound on the number of shots set by the s_j value for the parameter θ_j

Algorithm 1 Stochastic gradient descent with iCANS1/2. The function $iEvaluate(\boldsymbol{\theta}, \mathbf{s})$ evaluates the gradient at $\boldsymbol{\theta}$ using s_i measurements for the i -th derivative and returns the estimated gradient vector \mathbf{g} as well as the vector \mathbf{S} with the variances of the individual estimates of the partial derivatives.

Input: Learning rate α , starting point $\boldsymbol{\theta}_0$, min number of shots per estimation s_{\min} , number of shots that can be used in total N , Lipschitz constant L , running average constant μ , bias for gradient norm b

```

1: initialize:  $\boldsymbol{\theta} \leftarrow \boldsymbol{\theta}_0$ ,  $s_{\text{tot}} \leftarrow 0$ ,  $\mathbf{s} \leftarrow (s_{\min}, \dots, s_{\min})^T$ ,  $\boldsymbol{\chi} \leftarrow (0, \dots, 0)^T$ ,  $\boldsymbol{\xi} \leftarrow (0, \dots, 0)^T$ ,  $k \leftarrow 0$ 
2: while  $s_{\text{tot}} < N$  do
3:    $\mathbf{g}, \mathbf{S} \leftarrow iEvaluate(\boldsymbol{\theta}, \mathbf{s})$ 
4:    $s_{\text{tot}} \leftarrow s_{\text{tot}} + 2 \sum_i s_i$ 
5:    $\boldsymbol{\xi} \leftarrow \mu \boldsymbol{\xi} + (1 - \mu) \mathbf{S}$ 
6:    $\boldsymbol{\chi} \leftarrow \mu \boldsymbol{\chi} + (1 - \mu) \mathbf{g}$ 
7:   for  $i \in [1, \dots, d]$  do
8:     if iCANS1 then
9:        $\boldsymbol{\theta}_i \leftarrow \boldsymbol{\theta}_i - \alpha \mathbf{g}_i$ 
10:    else if iCANS2 then
11:      if  $\alpha \leq \frac{\chi_i^2}{L(\chi_i^2 + \xi_i/s_i)}$  then
12:         $\boldsymbol{\theta}_i \leftarrow \boldsymbol{\theta}_i - \alpha \mathbf{g}_i$ 
13:      else
14:         $\alpha' \leftarrow \frac{\chi_i^2}{L(\chi_i^2 + \xi_i/s_i)}$ 
15:         $\boldsymbol{\theta}_i \leftarrow \boldsymbol{\theta}_i - \alpha' \mathbf{g}_i$ 
16:      end if
17:    end if
18:     $s_i \leftarrow \left\lceil \frac{2L\alpha}{2-L\alpha} \frac{\xi_i}{\chi_i^2 + b\mu^k} \right\rceil$ 
19:     $\gamma_i \leftarrow \frac{1}{s_i} \left[ \left( \alpha - \frac{L\alpha^2}{2} \right) \chi_i^2 - \frac{L\alpha^2}{2s_i} \xi_i \right]$ 
20:  end for
21:   $s_{\max} \leftarrow s_{\arg \max_i \gamma_i}$ 
22:   $\mathbf{s} \leftarrow clip(\mathbf{s}, s_{\min}, s_{\max})$ 
23:   $k \leftarrow k + 1$ 
24: end while
```

that has the highest expected gain per shot, γ_i . In other words:

$$s_{\max} = s_{i_{\max}}, \quad (20)$$

$$i_{\max} := \arg \max_i \frac{\mathbb{E}[\mathcal{G}_i]}{s_i}. \quad (21)$$

We note that the introduction of this upper bound is a heuristic choice which we find to often be beneficial to shot frugality, but which removes the guarantee that the expected gain for an iteration will be positive. In order to preserve this frugality while retaining the guarantee, one can also introduce a step that verifies that the learning rate to be used is appropriate after the measurements are taken and adapts it if it is not. Motivated by (12), we check the following condition for each component of the gradient:

$$\alpha \leq \frac{g_i^2}{L(g_i^2 + S_i/s_i)}. \quad (22)$$

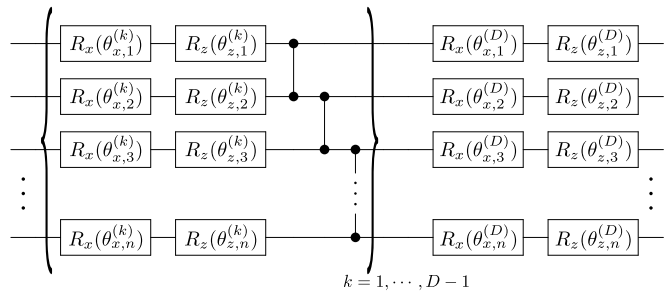


Figure 1. The quantum circuit diagram for the ansatz we used to construct the unitary operator $U(\boldsymbol{\theta})$. We note that this is the same ansatz used in Ref. [33].

When this condition fails to hold for the i -th partial derivative, we temporarily replace α with the right hand side of (22) for the update along that direction. Adding in this check results in a more conservative procedure as it enforces that $\mathbb{E}[\mathcal{G}_i] > 0$, and thus restores the guarantee that $\mathbb{E}[\mathcal{G}] > 0$. Below, we will refer to iCANS without this learning rate check as iCANS1 and with it as iCANS2. The distinction between iCANS1 and iCANS2 is made in Algorithm 1 with the conditional statements on lines 8 and 10.

IV. IMPLEMENTATIONS

In order to compare the performance of iCANS1 and iCANS2 to established methods, we consider two optimization tasks: variational quantum compiling with a fixed input state [14–17] and a variational quantum eigensolver (VQE) [3] for a Heisenberg spin chain.

In the iCANS implementations (see Algorithm 1) we use exponential moving averages for the estimates of the gradients and the variance. To ensure numerical stability, we add a bias b to the norm of the components of the gradient, which is then decayed exponentially. For our experiments we set the hyperparameters as $\alpha = 0.1$, $\mu = 0.99$, and $b = 10^{-6}$.

For the other algorithms we compare to, we will denote the number of shots per operator measurement as s . We will denote algorithm A with s shots per operator measurement as A- s (e.g., SOFF with $s = 1000$ is denoted SOFF-1000).

A. Variational Compiling with a Fixed Input State

For our first optimization task, we follow [33] and consider as a benchmark the optimization of the following cost function:

$$C = 1 - |\langle \mathbf{0} | U(\boldsymbol{\theta}^*)^\dagger U(\boldsymbol{\theta}) | \mathbf{0} \rangle|^2 \quad (23)$$

where $\boldsymbol{\theta}^*$ is a vector of fixed, randomly selected angles and $\boldsymbol{\theta}$ is the vector of angles to be optimized over. For

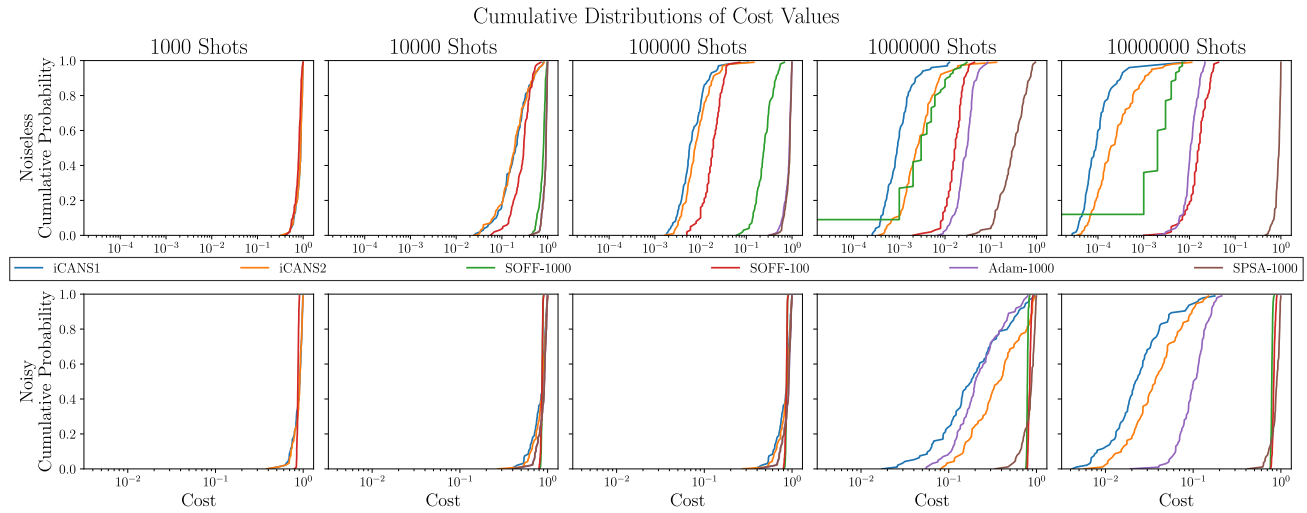


Figure 2. Cumulative probability distributions of the cost function values obtained while performing the fixed input state compilation optimization task with $n=3$ qubits and various optimizers after different numbers of shots. Note that the further to the left a curve is, the better the optimizer has minimized the cost. The top row shows the results for the case of no noise while the bottom row shows the noisy case. Each optimizer was given the same set of one hundred random seeds to allow for a more direct comparison. We show SOFF run with both $s = 1000$ and $s = 100$ (SOFF-1000 and SOFF-100 respectively), as well as both SPSA and Adam algorithms with $s = 1000$. Note that we do not show the optimizers with $s = 1000$ on the plots with $N = 1000$ total shots.

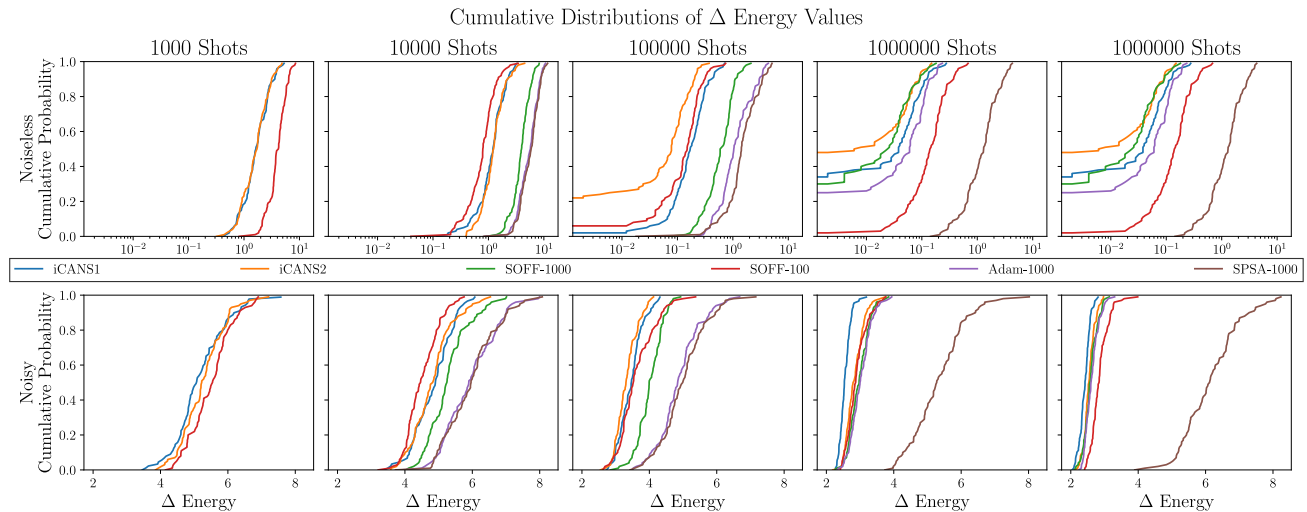


Figure 3. Cumulative probability distribution of the energy obtained while running a VQE procedure on a Heisenberg spin chain with $n=3$ qubits and various optimizers after different numbers of shots. Note that the further to the left a curve is, the better the optimizer has minimized the energy. The x axis shows the difference between the energy achieved by the optimizer and the exact optimizer ground state energy. The top row shows the the optimizer results for the case of no noise while the bottom row shows the noisy case. Note that, due to the relevant scales, we have made the x axis for the noisy case linear rather than logarithmic as in the other cases. Each optimizer was given the same set of one hundred random seeds to allow for a more direct comparison. We show SOFF run with both $s = 1000$ and $s = 100$ (SOFF-1000 and SOFF-100 respectively), as well as both SPSA and Adam algorithms with $s = 1000$. Note that we do not show the optimizers with $s = 1000$ on the plots with $N = 1000$ total shots.

this problem, we construct the parametrized unitary operator $U(\theta)$ with the ansatz described in Fig. 1, setting $n = 3$ qubits and $D = 6$. We then simulate the optimization procedure with one hundred different random

seeds and a collection of different optimizers. The results for both the case of a noiseless simulator and the case of a simulator using the noise profile of IBM's Melbourne processor [52] are shown in Fig. 2. For the latter, we em-

TABLE I. Noiseless Compilation Average Cost Values

# Shots	10^3	10^4	10^5	10^6	10^7
iCANS1	0.71506	0.03895	0.00397	0.00058	0.00009
iCANS2	0.71115	0.04051	0.00844	0.00182	0.00020
SOFF-1000	X	0.64767	0.04331	0.00232	0.00232
SOFF-100	0.66364	0.06261	0.01769	0.01707	0.01707
Adam-1000	X	0.87407	0.45529	0.01135	0.01135
SPSA-1000	X	0.87607	0.73053	0.12487	0.97404
Best	SOFF-100	iCANS1	iCANS1	iCANS1	iCANS1

TABLE III. Noiseless VQE Average Energies

# Shots	10^3	10^4	10^5	10^6	10^7
iCANS1	-4.12128	-4.71516	-5.79682	-5.96500	-5.96500
iCANS2	-4.17816	-4.64758	-5.92248	-5.99454	-5.99454
SOFF-1000	X	-1.92184	-5.32214	-5.97750	-5.97750
SOFF-100	-1.80458	-5.11828	-5.84480	-5.83050	-5.83050
Adam-1000	X	-0.35158	-4.62036	-5.94642	-5.94642
SPSA-1000	X	-0.09160	-4.25534	-4.54372	-4.54372
Best	iCANS2	SOFF-100	iCANS2	iCANS2	iCANS2

phasize that this noise profile reflects the properties of real, currently available quantum hardware. In addition, the average costs obtained for each optimizer as well as the optimizer that found the lowest cost on average for each number of shots (labeled “Best”) are listed in Tables I and II.

B. VQE

For our second optimization task, we follow [49] in considering the Heisenberg spin chain with wrapped boundary conditions and the Hamiltonian:

$$H = J \sum_{\langle ij \rangle} (X_i X_j + Y_i Y_j + Z_i Z_j) + B \sum_i Z_i, \quad (24)$$

where the $\langle \rangle$ bracket denotes nearest-neighbor pairs. For the purpose of our comparison, we fix $J = 1$ and $B = 3$ and again consider the ansatz described in Fig. 1. Running the comparison with $n = 3$ qubits in a triangle and $D = 6$ for the ansatz, we simulate running VQE with one hundred different random seeds and the same set of optimizers as in the benchmark case above. As before, the results for the both a noiseless and a noisy simulator (also using the IBM Melbourne processor’s noise profile [52]) are shown in Fig. 3. Again, the average energies obtained for each optimizer as well as the optimizer that found the lowest energy on average for each number of shots are listed in Tables III and IV.

TABLE II. Noisy Compilation Average Cost Values

# Shots	10^3	10^4	10^5	10^6	10^7
iCANS1	0.86522	0.67702	0.67702	0.08988	0.02274
iCANS2	0.87220	0.71458	0.71458	0.18643	0.02963
SOFF-1000	X	0.85707	0.85707	0.78834	0.78834
SOFF-100	0.86796	0.84264	0.84264	0.83146	0.83146
Adam-1000	X	0.88065	0.88065	0.10595	0.10595
SPSA-1000	X	0.88057	0.88057	0.76600	0.87527
Best	iCANS1	iCANS1	iCANS1	iCANS1	iCANS1

TABLE IV. Noisy VQE Average Energies

# Shots	10^3	10^4	10^5	10^6	10^7
iCANS1	-0.85013	-1.16663	-2.54836	-3.44440	-3.58782
iCANS2	-0.74114	-1.18706	-2.67302	-3.16188	-3.45476
SOFF-1000	X	-0.71950	-1.98712	-3.03234	-3.41642
SOFF-100	-0.50854	-1.49302	-2.38110	-3.10174	-3.14592
Adam-1000	X	-0.06516	-1.11762	-2.98332	-3.37674
SPSA-1000	X	-0.03862	-1.00830	-0.68360	0.13418
Best	iCANS1	SOFF-100	iCANS2	iCANS1	iCANS1

V. DISCUSSION

For the fixed-input compilation task (Fig. 2), it appears that both iCANS1 and iCANS2 performed comparably or better than the other optimizers considered for any given number of shots (see Tables I and II). We note that the SOFF algorithm also performed well in the noiseless case, and was the best for $N = 10^3$ with $m = 100$. When $s = 1000$, the SOFF algorithm appears to have approached a steady distribution for $N = 10^6$ and $N = 10^7$ which includes some probability achieving essentially zero cost, though in these cases iCANS still performed better on average. It is worth noting that when going from $N = 10^6$ to $N = 10^7$ the cost distribution for SOFF did not change while iCANS continued to improve.

iCANS1 and iCANS2 stood out more strongly in the noisy case as, other than Adam, the other optimizers did not improve significantly as N increased. Adam was competitive up to $N = 10^6$ but then did not continue improving, showing that the iCANS methods were the most noise resilient for this task. We emphasize that since the circuit depth for the compilation is roughly double the depth for the VQE case (as we have two repetitions of the unitary structure in Fig. 1), this task was our strongest test of noise resilience. We also note that in both the noisy and noiseless cases of this task, the more aggressive variant, iCANS1, seems to have outperformed the more conservative iCANS2.

Looking to the VQE case we studied (Fig. 3), we again find both iCANS1 and iCANS2 to be comparable or better to the other optimizers considered (see Tables III and IV). Again, we find the SOFF algorithm in particular also

performed fairly well for the noiseless case and note that it does not seem to have struggled in the noisy case the way it did for the compilation example. In fact, SOFF with $s = 100$ for $N = 10^4$ total shots performed the best for both the noisy and noiseless case (with the iCANS algorithms in second and third) and came in between iCANS2 and iCANS1 for $N = 10^5$ total shots for the noiseless case. We also note that for the noiseless case with either $N = 10^6$ or $N = 10^7$ shots, SOFF given $s = 1000$ performed slightly better than iCANS1, though iCANS2 (the more conservative algorithm) did the best.

Taking together all of the data in Tables I – IV, the iCANS algorithms performed the best on average. In addition, comparing iCANS1 and iCANS2 we find that the more aggressive iCANS1 often performed better, but that for the noisy VQE case the more conservative iCANS2 did significantly better. We expect that the better of the two will be highly problem dependent, but note that iCANS2 usually seems to be a safe choice.

We remark that while we do not report full results for RAdam [47], we found with preliminary results that it did not seem to provide a substantial improvement over the simpler Adam algorithm for our use cases. The latter was always out-performed by, e.g., iCANS1.

VI. CONCLUSIONS

In order to bring about the promise of VHQCs solving usefully large and complex problems on NISQ devices, one needs a way to perform the requisite optimizations efficiently. As the rate-limiting step of these optimizations will likely be the number of times one must prepare and measure quantum states, it will be important to have optimizers that are frugal in the number of times physical measurements must be performed on a quantum computer.

In this work we introduced two versions of a measurement-frugal, noise-resilient optimizer tailored for VHQCs. Both of the strategies we propose, iCANS1 and iCANS2, address measurement frugality by dynamically determining the number of measurements needed for each partial derivative of each step in a gradient descent. iCANS1 is the more aggressive version, always taking the same learning rate, while iCANS2 is more cautious and limits the learning rate for steps so that the expected gain is always guaranteed to be positive. Our numerical results indicate that these optimizers typically perform comparably or better than other state-of-the-art optimizers. The performance compares especially well in the presence of realistic hardware noise.

One potential direction for future work is exploring the possibility of extending our frugal adaptive approach to non-gradient methods, such as SPSA.

ACKNOWLEDGMENTS

JMK acknowledges support from the U.S. Department of Energy (DOE) through a quantum computing program sponsored by the Los Alamos National Laboratory (LANL) Information Science & Technology Institute. AA, LC, and PJC acknowledge support from the LDRD program at LANL. PJC also acknowledges support from the LANL ASC Beyond Moore’s Law project. This work was also supported by the U.S. DOE, Office of Science, Office of Advanced Scientific Computing Research, under the Quantum Computing Application Teams program.

VII. REFERENCES

- [1] John Preskill, “Quantum computing in the NISQ era and beyond,” *Quantum* **2**, 79 (2018).
- [2] Jarrod R McClean, Jonathan Romero, Ryan Babbush, and Alán Aspuru-Guzik, “The theory of variational hybrid quantum-classical algorithms,” *New Journal of Physics* **18**, 023023 (2016).
- [3] Alberto Peruzzo, Jarrod McClean, Peter Shadbolt, Man-Hong Yung, Xiao-Qi Zhou, Peter J Love, Alán Aspuru-Guzik, and Jeremy L O’Brien, “A variational eigenvalue solver on a photonic quantum processor,” *Nature Communications* **5**, 4213 (2014).
- [4] Edward Farhi, Jeffrey Goldstone, and Sam Gutmann, “A quantum approximate optimization algorithm,” *arXiv:1411.4028* (2014).
- [5] Peter D Johnson, Jonathan Romero, Jonathan Olson, Yudong Cao, and Alán Aspuru-Guzik, “QVECTOR: an algorithm for device-tailored quantum error correction,” *arXiv:1711.02249* (2017).
- [6] Jonathan Romero, Jonathan P Olson, and Alan Aspuru-Guzik, “Quantum autoencoders for efficient compression of quantum data,” *Quantum Science and Technology* **2**, 045001 (2017).
- [7] Ryan LaRose, Arkin Tikku, Étude O’Neel-Judy, Lukasz Cincio, and Patrick J Coles, “Variational quantum state diagonalization,” *npj Quantum Information* **5**, 57 (2019).
- [8] Andrew Arrasmith, Lukasz Cincio, Andrew T Sornborger, Wojciech H Zurek, and Patrick J Coles, “Variational consistent histories as a hybrid algorithm for quantum foundations,” *Nature Communications* **10**, 3438 (2019).
- [9] M Cerezo, Alexander Poremba, Lukasz Cincio, and Patrick J Coles, “Variational quantum fidelity estimation,” *arXiv:1906.09253* (2019).
- [10] Tyson Jones, Suguru Endo, Sam McArdle, Xiao Yuan, and Simon C Benjamin, “Variational quantum algorithms for discovering hamiltonian spectra,” *Physical Review A* **99**, 062304 (2019).
- [11] Xiao Yuan, Suguru Endo, Qi Zhao, Simon Benjamin, and Ying Li, “Theory of variational quantum simulation,” *arXiv:1812.08767* (2018).
- [12] Ying Li and Simon C Benjamin, “Efficient variational quantum simulator incorporating active error minimization,” *Physical Review X* **7**, 021050 (2017).
- [13] C Kokail, C Maier, R van Bijnen, T Brydges, MK Joshi, P Jurcevic, CA Muschik, P Silvi, R Blatt, CF Roos,

- et al.*, “Self-verifying variational quantum simulation of lattice models,” *Nature* **569**, 355 (2019).
- [14] Sumeet Khatry, Ryan LaRose, Alexander Poremba, Lukasz Cincio, Andrew T Sornborger, and Patrick J Coles, “Quantum-assisted quantum compiling,” *Quantum* **3**, 140 (2019).
- [15] Tyson Jones and Simon C Benjamin, “Quantum compilation and circuit optimisation via energy dissipation,” *arXiv:1811.03147* (2018).
- [16] Kentaro Heya, Yasunari Suzuki, Yasunobu Nakamura, and Keisuke Fujii, “Variational quantum gate optimization,” *arXiv:1810.12745* (2018).
- [17] Kunal Sharma, Sumeet Khatry, M Cerezo, and Patrick J Coles, “Noise resilience of variational quantum compiling,” *arXiv:1908.04416* (2019).
- [18] Jacques Carolan, Masoud Mosheni, Jonathan P Olson, Mihika Prabhu, Changchen Chen, Darius Bunandar, Nicholas C Harris, Franco NC Wong, Michael Hochberg, Seth Lloyd, *et al.*, “Variational quantum unsampling on a quantum photonic processor,” *arXiv:1904.10463* (2019).
- [19] Nobuyuki Yoshioka, Yuya O Nakagawa, Kosuke Mitarai, and Keisuke Fujii, “Variational quantum algorithm for non-equilibrium steady states,” *arXiv:1908.09836* (2019).
- [20] Carlos Bravo-Prieto, LaRose, M. Cerezo, Yigit Subasi, Lukasz Cincio, and Patrick J. Coles, “Variational quantum linear solver: A hybrid algorithm for linear systems,” *arXiv:1909.05820* (2019).
- [21] Dave Wecker, Matthew B Hastings, and Matthias Troyer, “Progress towards practical quantum variational algorithms,” *Phys. Rev. A* **92**, 042303 (2015).
- [22] Yudong Cao, Jonathan Romero, Jonathan P Olson, Matthias Degroote, Peter D Johnson, Mária Kieferová, Ian D Kivlichan, Tim Menke, Borja Peropadre, Nicolas PD Sawaya, *et al.*, “Quantum chemistry in the age of quantum computing,” *Chemical reviews* (2018).
- [23] Sam McArdle, Suguru Endo, Alan Aspuru-Guzik, Simon Benjamin, and Xiao Yuan, “Quantum computational chemistry,” *arXiv:1808.10402* (2018).
- [24] Andrew Jena, Scott Genin, and Michele Mosca, “Pauli partitioning with respect to gate sets,” *arXiv:1907.07859* (2019).
- [25] Artur F Izmaylov, Tzu-Ching Yen, Robert A Lang, and Vladyslav Verteletskyi, “Unitary partitioning approach to the measurement problem in the variational quantum eigensolver method,” *arXiv:1907.09040* (2019).
- [26] Tzu-Ching Yen, Vladyslav Verteletskyi, and Artur F Izmaylov, “Measuring all compatible operators in one series of a single-qubit measurements using unitary transformations,” *arXiv:1907.09386* (2019).
- [27] Pranav Gokhale, Olivia Angiuli, Yongshan Ding, Kaiwen Gui, Teague Tomesh, Martin Suchara, Margaret Martonosi, and Frederic T Chong, “Minimizing state preparations in variational quantum eigensolver by partitioning into commuting families,” *arXiv:1907.13623* (2019).
- [28] Ophelia Crawford, Barnaby van Straaten, Daochen Wang, Thomas Parks, Earl Campbell, and Stephen Brierley, “Efficient quantum measurement of pauli operators,” *arXiv:1908.06942* (2019).
- [29] Pranav Gokhale and Frederic T Chong, “ $o(n^3)$ measurement cost for variational quantum eigensolver on molecular hamiltonians,” *arXiv:1908.11857* (2019).
- [30] William J Huggins, Jarrod McClean, Nicholas Rubin, Zhang Jiang, Nathan Wiebe, K Birgitta Whaley, and Ryan Babbush, “Efficient and noise resilient measurements for quantum chemistry on near-term quantum computers,” *arXiv:1907.13117* (2019).
- [31] Guillaume Verdon, Michael Broughton, Jarrod R McClean, Kevin J Sung, Ryan Babbush, Zhang Jiang, Hartmut Neven, and Masoud Mohseni, “Learning to learn with quantum neural networks via classical neural networks,” *arXiv:1907.05415* (2019).
- [32] Max Wilson, Sam Stromswold, Filip Wudarski, Stuart Hadfield, Norm M Tubman, and Eleanor Rieffel, “Optimizing quantum heuristics with meta-learning,” *arXiv:1908.03185* (2019).
- [33] Ken M Nakanishi, Keisuke Fujii, and Synge Todo, “Sequential minimal optimization for quantum-classical hybrid algorithms,” *arXiv:1903.12166* (2019).
- [34] Robert M Parrish, Joseph T Iosue, Asier Ozaeta, and Peter L McMahon, “A Jacobi diagonalization and Anderson acceleration algorithm for variational quantum algorithm parameter optimization,” *arXiv:1904.03206* (2019).
- [35] James Stokes, Josh Izaac, Nathan Killoran, and Giuseppe Carleo, “Quantum natural gradient,” *arXiv:1909.02108* (2019).
- [36] Lukas Balles, Javier Romero, and Philipp Hennig, “Coupling Adaptive Batch Sizes with Learning Rates,” in *Proceedings of the Thirty-Third Conference on Uncertainty in Artificial Intelligence (UAI)* (2017) pp. 410–419.
- [37] Gadi Aleksandrowicz *et al.*, “Qiskit: An Open-source Framework for Quantum Computing,” (2019).
- [38] Diederik P Kingma and Jimmy Ba, “Adam: A method for stochastic optimization,” in *Proceedings of the 3rd International Conference on Learning Representations (ICLR)* (2015).
- [39] James C Spall, “Multivariate stochastic approximation using a simultaneous perturbation gradient approximation,” *IEEE transactions on automatic control* **37**, 332–341 (1992).
- [40] Yann LeCun, Yoshua Bengio, and Geoffrey Hinton, “Deep learning,” *Nature* **521**, 436 (2015).
- [41] Kosuke Mitarai, Makoto Negoro, Masahiro Kitagawa, and Keisuke Fujii, “Quantum circuit learning,” *Phys. Rev. A* **98**, 032309 (2018).
- [42] Maria Schuld, Ville Bergholm, Christian Gogolin, Josh Izaac, and Nathan Killoran, “Evaluating analytic gradients on quantum hardware,” *Phys. Rev. A* **99**, 032331 (2019).
- [43] Ville Bergholm, Josh Izaac, Maria Schuld, Christian Gogolin, and Nathan Killoran, “Pennylane: Automatic differentiation of hybrid quantum-classical computations,” *arXiv:1811.04968* (2018).
- [44] Aram Harrow and John Napp, “Low-depth gradient measurements can improve convergence in variational hybrid quantum-classical algorithms,” *arXiv:1901.05374* (2019).
- [45] Gian Giacomo Guerreschi and Mikhail Smelyanskiy, “Practical optimization for hybrid quantum-classical algorithms,” *arXiv:1701.01450* (2017).
- [46] James S Bergstra, Rémi Bardenet, Yoshua Bengio, and Balázs Kégl, “Algorithms for hyper-parameter optimization,” in *Advances in Neural Information Processing Systems 24* (2011) pp. 2546–2554.
- [47] Liyuan Liu, Haoming Jiang, Pengcheng He, Weizhu Chen, Xiaodong Liu, Jianfeng Gao, and Jiawei Han, “On the variance of the adaptive learning rate and beyond,” *arXiv:1908.03265* (2019).
- [48] James C Spall, “Implementation of the simultaneous per-

- turbation algorithm for stochastic optimization,” *IEEE Transactions on aerospace and electronic systems* **34**, 817–823 (1998).
- [49] Abhinav Kandala, Antonio Mezzacapo, Kristan Temme, Maika Takita, Markus Brink, Jerry M Chow, and Jay M Gambetta, “Hardware-efficient variational quantum eigensolver for small molecules and quantum magnets,” *Nature* **549**, 242 (2017).
- [50] Michael JD Powell, “An efficient method for finding the minimum of a function of several variables without calculating derivatives,” *The Computer Journal* **7**, 155–162 (1964).
- [51] Richard P Brent, *Algorithms for Minimization Without Derivatives* (Dover Publications, 2013).
- [52] “IBM Q 16 Melbourne backend specification,” <https://github.com/Qiskit/ibmq-device-information/tree/master/backends/melbourne/V1> (2018).

Appendix A: CANS Algorithm

For the interested reader, we present the algorithm for CANS (Coupled Adaptive Number of Shots) in Algorithm 2, which is an adaptation of the CABS algorithm [36] to the VHQCA setting.

Algorithm 2 Stochastic gradient descent with CANS. The function $Evaluate(\boldsymbol{\theta}, s)$ evaluates the gradient at $\boldsymbol{\theta}$ using s measurements for each component of the derivative and returns the estimated gradient vector \mathbf{g} as well as the vector \mathbf{S} with the variances of the individual estimates of the partial derivatives.

Input: Learning rate α , starting point $\boldsymbol{\theta}_0$, min number of shots per estimation s_{\min} , number of shots that can be used in total N , Lipschitz constant L , running average constant μ , bias for gradient norm b

- 1: initialize: $\boldsymbol{\theta} \leftarrow \boldsymbol{\theta}_0$, $s_{\text{tot}} \leftarrow 0$, $s \leftarrow s_{\min}$, $\boldsymbol{\chi} \leftarrow (0, \dots, 0)^T$, $\xi \leftarrow 0$, $k \leftarrow 0$
- 2: **while** $s_{\text{tot}} < N$ **do**
- 3: $\mathbf{g}, \mathbf{S} \leftarrow Evaluate(\boldsymbol{\theta}, s)$
- 4: $s_{\text{tot}} \leftarrow s_{\text{tot}} + 2s$
- 5: $\boldsymbol{\theta} \leftarrow \boldsymbol{\theta} - \alpha \boldsymbol{\theta}$
- 6: $\xi \leftarrow \mu \xi + (1 - \mu) \|\mathbf{S}\|_1$
- 7: $\boldsymbol{\chi} \leftarrow \mu \boldsymbol{\chi} + (1 - \mu) \mathbf{g}$
- 8: $s \leftarrow \left\lceil \frac{2L\alpha}{2-L\alpha} \frac{\xi}{\|\boldsymbol{\chi}\|^2 + b\mu^k} \right\rceil$
- 9: $s \leftarrow \max(s, s_{\min})$
- 10: $k \leftarrow k + 1$
- 11: **end while**
